# Population of the $2^+_{ms}$ mixed-symmetry state of $^{140}$Ba with the $\alpha$-transfer reaction

C. Stahl,[1,*] J. Leske,[1] C. Bauer,[1] D. Bazzacco,[2] E. Farnea,[2,†] A. Gottardo,[3,4] P. R. John,[1,‡] C. Michelagnoli,[3,2,§] N. Pietralla,[1] M. Reese,[1] E. Şahin,[4,‖] B. Birkenbach,[5] A. Bracco,[6,7] F. C. L. Crespi,[6,7] G. de Angelis,[4] P. Désesquelles,[8] J. Eberth,[5] A. Gadea,[9] A. Görgen,[10,11,§] J. Grebosz,[12] H. Hess,[5] J. Jolie,[5] A. Jungclaus,[13] W. Korten,[10] S. M. Lenzi,[3,2] S. Lunardi,[3,2] R. Menegazzo,[2] D. Mengoni,[14,¶] V. Modamio,[4,‡] D. R. Napoli,[4] A. Pullia,[6,7] B. Quintana,[15] F. Recchia,[3,2] P. Reiter,[5] D. Rosso,[4] M. D. Salsac,[10] P.-A. Söderström,[16,17] O. Stezowski,[18] Ch. Theisen,[10] C. A. Ur,[2,**] and J. J. Valiente-Dobón[4]

[1]*Institut für Kernphysik, Technische Universität Darmstadt, D-64291 Darmstadt, Germany*
[2]*Istituto Nazionale di Fisica Nucleare, Sezione di Padova, I-35131 Padova, Italy*
[3]*Dipartimento di Fisica e Astronomia, Università di Padova, I-35131 Padova, Italy*
[4]*Istituto Nazionale di Fisica Nucleare, Laboratori Nazionali di Legnaro, I-35020 Legnaro, Italy*
[5]*Institut für Kernphysik, Universität zu Köln, Zülpicher Straße 77, D-50937 Köln, Germany*
[6]*Dipartimento di Fisica, Università degli Studi di Milano, I-20133 Milano, Italy*
[7]*Istituto Nazionale di Fisica Nucleare, Sezione di Milano, I-20133 Milano, Italy*
[8]*Centre de Spectrométrie Nucléaire et de Spectrométrie de Masse CSNSM, CNRS/IN2P3 and Université Paris-Sud, F-91405 Orsay Campus, France*
[9]*Instituto de Física Corpuscular, CSIC-Universitat de València, E-46980 València, Spain*
[10]*Institut de Recherche sur les lois Fondamentales de l'Univers IRFU, CEA/DSM, Centre CEA de Saclay, F-91191 Gif-sur-Yvette Cedex, France*
[11]*Department of Physics, University of Oslo, P.O. Box 1048 Blindern, N-0316 Oslo, Norway*
[12]*The Henryk Niewodniczański Institute of Nuclear Physics, Polish Academy of Sciences, ul. Radzikowskiego 152, 31-342 Kraków, Poland*
[13]*Instituto de Estructura de la Materia, CSIC, Madrid, E-28006 Madrid, Spain*
[14]*Nuclear Physics Research Group, University of the West of Scotland, High Street, Paisley, PA1 2BE Scotland, United Kingdom*
[15]*Laboratorio de Radiaciones Ionizantes, Departamento de Fsica Fundamental, Universidad de Salamanca, E-37008 Salamanca, Spain*
[16]*Department of Physics and Astronomy, Uppsala University, SE-75120 Uppsala, Sweden*
[17]*RIKEN Nishina Center, 2-1 Hirosawa, Wako, 351-0198 Saitama, Japan*
[18]*Université de Lyon, CNRS-IN2P3, Institut de Physique Nucléaire de Lyon, F-69622 Villeurbanne, France*

(Received 11 September 2015; published 26 October 2015)

**Background:** Identification of proton-neutron mixed-symmetric one-quadrupole phonon excitations (the $2^+_{ms}$ states) of atomic nuclei provides information on the isovector part of the residual nucleon-nucleon interaction. It was predicted that the $2^+_{ms}$ state of particular nuclei close to the U(5) limit of the interacting boson model, in particular $^{140}$Ba, should be considerably populated by $\alpha$-transfer reactions [C. E. Alonso *et al.*, Phys. Rev. C **78**, 017301 (2008)].

**Purpose:** We aim at the identification of the $2^+_{ms}$ mixed-symmetry state (MSS) of radioactive $^{140}$Ba and investigate its population by the $\alpha$-transfer reaction as a suitable tool to selectively populate MSSs and as a potential new signature for its mixed-symmetric character.

**Method:** A $\gamma$-ray spectroscopy experiment was performed in inverse kinematics in order to populate the $2^+_{ms}$ state of $^{140}$Ba by $\alpha$-transfer from a $^{nat}$C target on $^{136}$Xe beam ions. The population of the candidate for the $2^+_{ms}$ state of $^{140}$Ba was measured relative to the population of the $2^+_1$ state.

**Results:** The candidate for the $2^+_{ms}$ state of $^{140}$Ba was populated by $\alpha$ transfer three times weaker than predicted. Another $2^+$ state that can be ruled out as the MSS was in turn as strongly populated by the $\alpha$ transfer as predicted for the MSS.

**Conclusions:** The relative population of $2^+$ states by $\alpha$-transfer cannot serve as a new signature for MSSs, since other $2^+$ states are also strongly populated. Nevertheless, the substantial population of the MSS candidate of $^{140}$Ba by $\alpha$ transfer qualifies this type of reaction as suitable tool to excite MSSs and study their electromagnetic decay properties.

DOI: 10.1103/PhysRevC.92.044324 PACS number(s): 21.10.Re, 21.60.Fw, 25.40.Hs

*stahl@ikp.tu-darmstadt.de
†Deceased.
‡Present address: Dipartimento di Fisica e Astronomia, Università degli Studi di Padova and Istituto Nazionale di Fisica Nucleare, Sezione di Padova, I-35131 Padova, Italy.
§Present address: GANIL, CEA/DSM-CNRS/IN2P3, F-14076 Caen, France.
‖Present address: Department of Physics, University of Oslo, P.O. Box 1048 Blindern, N-0316 Oslo, Norway.
¶Present address: Dipartimento di Fisica e Astronomia, Università di Padova and Istituto Nazionale di Fisica Nucleare, Sezione di Padova, I-35131 Padova, Italy.
**Present address: Extreme Light Infrastructure - Nuclear Physics Facility, MG-6 Bucharest Magurele, Romania.

 

## I. INTRODUCTION

Proton-neutron mixed-symmetry one-quadrupole phonon excitations, the $2^+_{\rm ms}$ states, are isovector valence-space excitations of even-even atomic nuclei [1,2]. They exist in (near-) spherical vibrators with a few pairs of protons and neutrons outside of doubly-closed shells and, in the framework of the proton-neutron version of the interacting boson model (IBM-2) [3], exhibit a nonmaximum $F$ spin [3,4] with $F = F_{\rm max} - 1$. In the same framework and the simple situation of one proton and one neutron boson, the one-phonon mixed-symmetry $2^+$ states $|2^+_{\rm ms}\rangle$ can be expressed as out-of-phase excitation of protons ($\pi$) and neutrons ($\nu$):

$$|2^+_{\rm ms}\rangle = \frac{1}{\sqrt{2}}(d^\dagger_\pi s^\dagger_\nu - s^\dagger_\pi d^\dagger_\nu)\,|0\rangle\,. \tag{1}$$

Here, $s^\dagger_{\pi\,(\nu)}$ and $d^\dagger_{\pi\,(\nu)}$ denote the proton (neutron) $s$- and $d$-boson creation operators, respectively. $|0\rangle$ denotes the boson-vacuum state. In contrast to the mixed-symmetric state defined in Eq. (1), the fully-symmetric one-quadrupole phonon state $|2^+_{\rm fs}\rangle$, i.e., the $2^+_1$ state of an even-even nucleus, is given by the respective in-phase excitation of protons and neutrons:

$$|2^+_{\rm fs}\rangle = \frac{1}{\sqrt{2}}(d^\dagger_\pi s^\dagger_\nu + s^\dagger_\pi d^\dagger_\nu)|0\rangle. \tag{2}$$

Equations (1) and (2) are valid in the U(5) limit of IBM-2, i.e., for spherical vibrators. The interest in mixed-symmetry states (MSSs) arises from their sensitivity to the proton-neutron part of the residual interaction $V_{pn}$ [5].

The prime experimental signature for $2^+_{\rm ms}$ states is their strong $M1$ decay to the fully-symmetric $2^+_1$ state with an absolute matrix element in the order of $\langle 2^+_{\rm ms}|\,M1\,|2^+_{\rm fs}\rangle \approx 1\mu_N$ and a weakly collective decay strength to the ground state of $B(E2, 2^+_{\rm ms} \rightarrow 0^+_1) \approx 1$ W.u. The strong $M1$ transition leads to short lifetimes of $2^+_{\rm ms}$ states in the order of 100 fs. In particular situations, alternative experimental signatures for $2^+_{\rm ms}$ states exist that are independent of their electromagnetic decay properties, for example the difference in transition radii of the $2^+_{\rm fs}$ and $2^+_{\rm ms}$ states [6]. Furthermore, Alonso *et al.* have investigated the population of $2^+_{\rm ms}$ states by $\alpha$-transfer reactions in the framework of IBM-2 [7]. They found that, in the U(5)-limit of spherical vibrators, the population of the $2^+_{\rm ms}$ state in $\alpha$-transfer reactions should be as strong as $1/3$ relative to the population of the $2^+_1$ state.

The first candidates for $2^+_{\rm ms}$ states were claimed in the $N = 84$ isotones $^{140}$Ba, $^{142}$Ce, and $^{144}$Sm based on the small $E2/M1$ multipole mixing ratio of their decays to the $2^+_1$ state [8]. In the stable nuclei $^{142}$Ce and $^{144}$Sm, the $2^+_{\rm ms}$ states were uniquely established by measurements of their absolute $B(M1)$ transition strengths to the $2^+_1$ states [9,10]. In radioactive $^{140}$Ba, however, the confirmation of the candidate $2^+$ state at 1993.7 keV as the $2^+_{\rm ms}$ state is still pending.

In the work of Alonso *et al.*, the nucleus $^{140}$Ba was identified as the ideal candidate for comparatively strong population of the $2^+_{\rm ms}$ state by $\alpha$ transfer from $^{12}$C nuclei [7]. Therefore, we conducted a $\gamma$-ray spectroscopy experiment in inverse kinematics aiming at the population of the $2^+_{\rm ms}$ state in radioactive $^{140}$Ba by the transfer of $\alpha$ particles from $^{12}$C target nuclei to a beam of $^{136}$Xe.

## II. EXPERIMENTAL DETAILS

In $\alpha$-transfer reactions, a $^4$He nucleus is exchanged between a projectile and a target nucleus. Although the details of $\alpha$-transfer reactions are not fully understood [7], it is well known that preferably low-spin states are excited in $\alpha$-transfer reactions [11] and that their cross sections are largest for swift collisions; i.e., for collisions where the distance of closest approach between projectile and target nuclei approximately equals the sum of their radii [12]. Therefore, the maximum cross section can be expected for beam energies just at the Coulomb barrier. At these beam energies, the $\alpha$ transfer will compete with Coulomb excitation and other transfer reactions as well as fusion-evaporation. Therefore, in our experiment, a clean identification of the $\alpha$-transfer reaction channel is mandatory. $\alpha$ transfer has been successfully used for the population of excited states in radioactive nuclei close to the valley of stability in several experiments, e.g., [13,14].

We have performed an experiment employing the inverse-kinematics reaction $^{12}$C($^{136}$Xe, $^{140}$Ba)$^8$Be at the Laboratori Nazionali di Legnaro (LNL) in order to populate excited states of the unstable nucleus $^{140}$Ba. A beam of $^{136}$Xe was provided by LNL's PIAVE/ALPI accelerator complex with an intensity of 0.5–1 pnA throughout the measurement. Runs were performed at two different beam energies of 500 and 546 MeV, respectively. The beam impinged on a self-supporting target made of $^{\rm nat}$C with a thickness of 0.915(11) mg/cm$^2$. Target-like reaction products were detected by an annular double-sided silicon-strip detector (DSSSD) with an inner (outer) active diameter of 32 (85) mm and a thickness of $\sim$300 $\mu$m. The DSSSD was placed at a distance of 33.4 mm downstream of the target and covered polar angles from $\theta_{p,<} = 25.6^\circ$ to $\theta_{p,>} = 51.8^\circ$ in the laboratory frame. The DSSSD was segmented into 32 rings in polar angle and 64 segments in azimuth angle, where always two adjacent azimuth segments were electrically combined resulting in 32 effective azimuth segments. $\gamma$ rays were observed with the AGATA demonstrator [15,16], consisting of 15 high-purity germanium crystals at the time of the measurement. The AGATA demonstrator was placed in backward direction and covered polar angles from $\theta_{\gamma,<} \approx 74^\circ$ to $\theta_{\gamma,>} \approx 164^\circ$. X rays and low-energy $\gamma$ rays where shielded by 1 mm copper and 2 mm lead plates in order to reduce the load of the data acquisition system. Data was recorded in particle-$\gamma$ coincidence mode. The reaction kinematics is shown in Fig. 1. It allows us to determine the velocity vectors of the beam-like reaction products from the polar and azimuth scattering angle of the target-like reaction products measured by the DSSSD on an event-by-event basis. These measured velocity vectors of the beam-like reaction products together with the positions of the first $\gamma$-ray interaction points in the AGATA detector crystals provided by the *adaptive grid search* algorithm for pulse shape analysis [17] and the *Orsay forward tracking* (OFT) algorithm [18] allow for a precise Doppler correction of the measured $\gamma$-ray energies.

### A. Reaction channel selection

The residual of the $^{12}$C target nuclei after an $\alpha$-transfer reaction, $^8$Be, is unstable and immediately breaks up into two

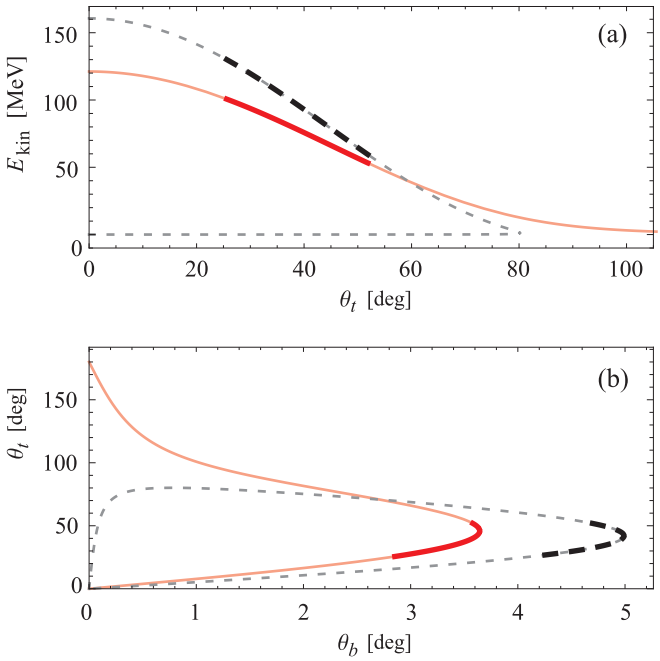


FIG. 1. (Color online) Reaction kinematics at 546 MeV beam energy for the $\alpha$-transfer reaction (red, solid line) and for Coulomb excitation (black, dashed line) for comparison. The polar-angular range covered by the DSSSD is indicated by the bold lines. (a) Kinetic energy $E_{kin}$ of the beam-like reaction product ($^{140}$Ba, $^{136}$Xe) plotted against the laboratory scattering angle $\theta_t$ of the target-like reaction product ($^{8}$Be, $^{12}$C). (b) Laboratory scattering angle $\theta_b$ of the beam-like reaction product plotted against the laboratory scattering angle $\theta_t$ of the target-like reaction product.

$\alpha$ particles with a $Q$ value of 91.8 keV. Since the kinetic energy of the target-like product $^{8}$Be is a function of its scattering angle in the laboratory system (see Fig. 1, top), also the maximum opening angle of the two $\alpha$ particles from the $^{8}$Be breakup is a function of the original $^{8}$Be scattering angle. This maximum opening angle is shown in Fig. 2. The coincident detection of two $\alpha$ particles at close distance is a clean signal for an $\alpha$-transfer reaction, since multiple $\alpha$ particles from other reactions such as fusion-evaporation do not exhibit this strong directional correlation.

The maximum separation of the two $\alpha$ particles once they impinge on the DSSSD is depicted in the inset of Fig. 2 for eight different scattering angles of the target-like reaction product $^{8}$Be. Two $\alpha$ particles from an $\alpha$-transfer reaction will always be detected in the same or in two adjacent azimuth segments of the DSSSD. In contrast, they may hit rings that are not directly adjacent. An add-back algorithm that combines energies coincidentally measured in adjacent rings or in adjacent segments of the DSSSD was applied. Therefore, the full sum-energy of two $\alpha$ particles from an $\alpha$-transfer reaction is always measured in the azimuth segments, but the energy of one of the $\alpha$ particles may be missed in the rings. The particle energies measured in one ring of the DSSSD at a beam energy of 546 MeV are plotted in Fig. 3 against the energies measured in any of the azimuth segments. The off-diagonal events in Fig. 3 represent the discussed case where the energy

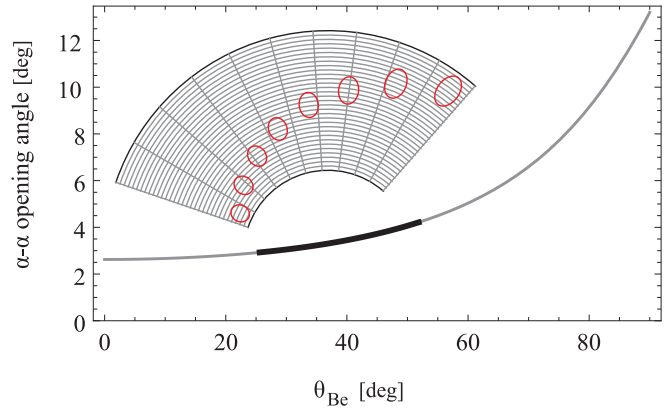


FIG. 2. (Color online) Maximum opening-angle of two $\alpha$ particles produced by the breakup of a $^{8}$Be nucleus, the target-like residual of an $\alpha$-transfer reaction (gray line). The opening angle is plotted against the laboratory scattering angle of the $^{8}$Be nucleus. The polar-angular range covered by the DSSSD is marked by the black, bold line. The two $\alpha$ particles are always detected in the same or in adjacent azimuth segments of the DSSSD, but may be detected in nonadjacent rings (the maximum separation of the two $\alpha$ particles for eight central emission angles of $^{8}$Be particles is depicted by the red ovals in the inset). The figure refers to 546 MeV beam energy.

of one of the two $\alpha$ particles from an $\alpha$-transfer reaction is missed by the add-back algorithm, because the particles hit two nonadjacent rings of the DSSSD.

The energies of the target-like reaction products at a given observation angle (or a given ring of the DSSSD) vary for the different occurring reactions, as exemplified in the top of Fig. 1. This allows us to separate the different reaction channels

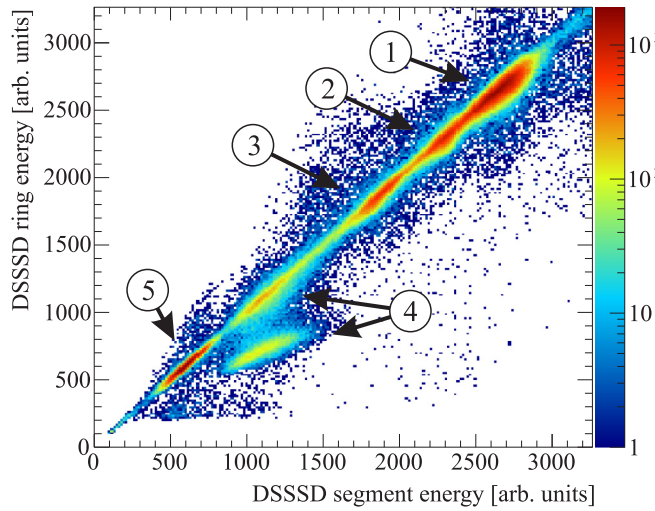


FIG. 3. (Color online) Spectrum of target-like particle energy measured in one ring of the DSSSD (covering $\theta_p = \{32.1°, \ldots, 33.1°\}$, $y$ axis) plotted against the energy measured in any of the azimuth segments ($x$ axis). Different reaction channels can clearly be separated. The events marked with ① correspond to Coulomb excitation, while the events marked with ④ correspond to $\alpha$ transfer. The other reactions are discussed in the text. Data taken at 546 MeV beam energy are shown.

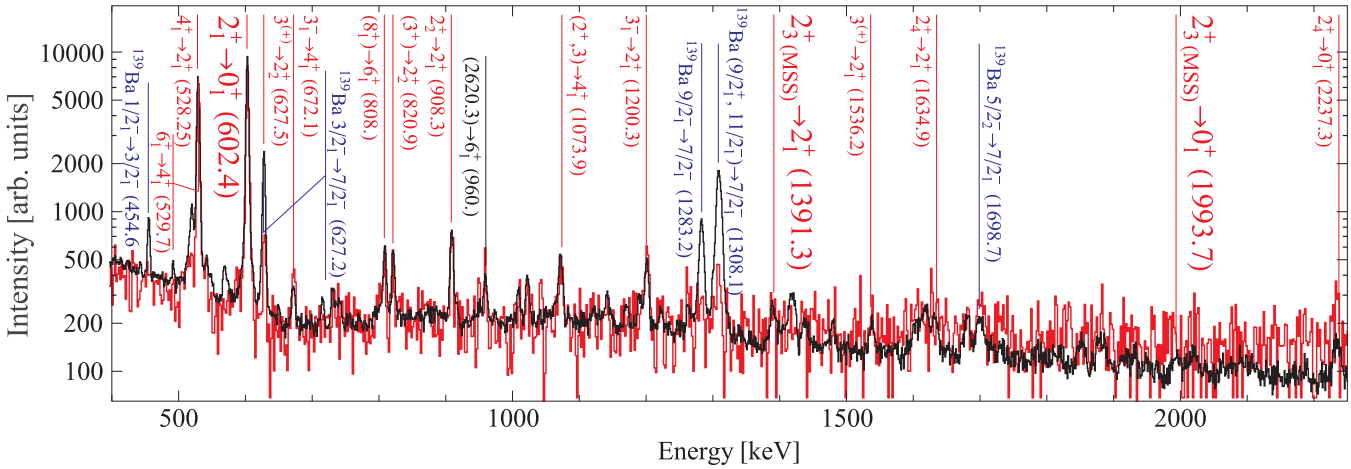


FIG. 4. (Color online) Doppler-corrected, random-subtracted $\gamma$-ray spectrum of $^{140}$Ba populated by $\alpha$ transfer. The spectra measured at 500 and 546 MeV beam energy are shown in red and black, respectively. Selection of events corresponding to $\alpha$ transfer is discussed in Sec. II A. The spectra are normalized such that they contain the same number of events in the $2_1^+ \rightarrow 0_1^+$ transition at 602.4 keV. For the 500 MeV spectrum, the content of each two adjacent bins was added in order to reduce fluctuations. Transitions in $^{140}$Ba are marked by red lines and labels, contaminating transitions are marked by blue lines and labels. The transition energies are taken from [19]. See text for details.

on an event-by-event basis as is clearly visible in Fig. 3. The separation is best at small laboratory scattering angles of the target-like reaction products (see Fig. 1 top).

By inspection of the corresponding $\gamma$-ray spectra, the events in Fig. 3 marked with ① can be identified with the Coulomb excitation of the $^{136}$Xe beam ions; the events marked with ④ correspond to $\alpha$-transfer reactions; and the events marked with ②, ③, and ⑤ are dominated by the reactions $^{12}$C($^{136}$Xe, $^{137}$Cs*)$^{11}$B (proton pick-up), $^{12}$C($^{136}$Xe, $^{138}$Ba*)$^{10}$Be (two-proton pick-up) and $^{12}$C($^{136}$Xe, $^{140}$Ba*)$2\alpha$ / $^{12}$C($^{136}$Xe, $^{142}$Ce*)$\alpha + 2n$ (fusion-evaporation reactions with $\alpha$ particles in the exit channel), respectively, as we could verify from the coincident $\gamma$-ray spectra. The analysis of the reaction channels other than $\alpha$ transfer will be discussed in forthcoming publications.

### B. $\gamma$-ray spectra

The $\gamma$-ray spectra corresponding to events where the occurrence of an $\alpha$-transfer reaction was identified (see previous subsection) are shown in Fig. 4 for both beam energies of 500 and 546 MeV. The spectrum is contaminated by transitions in the nucleus $^{139}$Ba that was presumably produced in the incomplete fusion reaction $^{12}$C($^{136}$Xe, $^{139}$Ba*)$\alpha + \alpha n$. In this reaction, the target carbon ions break up into an $\alpha$ particle and a $^{8}$Be nucleus. The latter fuses with the $^{136}$Xe beam ions. Excited states of $^{139}$Ba are then populated in the $\alpha n$ exit channel of the fusion product. In contrast to the evaporated $\alpha$ particles, the residual $\alpha$ particles from the $^{12}$C breakup are ejected with relatively high momentum and detected by the DSSSD at relatively high energy (see, e.g., [20] for another observation of incomplete fusion reactions under similar experimental conditions). These residual $\alpha$ particles exhibit kinetic energy similar to the two $\alpha$ particles from $\alpha$-transfer reactions together. Therefore, the incomplete fusion events cannot be distinguished from the $\alpha$-transfer events by the measured particle energy. In the particle spectra as shown in Fig. 3, they underlay the $\alpha$-transfer events for the case where the energy of both $\alpha$ particles has been measured (on-diagonal events in Fig. 3). It is clearly visible in Fig. 4 that the incomplete fusion reaction is strongly suppressed with respect to the $\alpha$-transfer reaction at the lower beam energy.

The statistics for the runs at 500 MeV beam energy is significantly lower since the duration of the measurement was much shorter than at 546 MeV beam energy. However, the decay pattern of $^{140}$Ba after $\alpha$ transfer and, hence, the $\alpha$-transfer excitation pattern is identical within the statistical uncertainties at both beam energies. This is visible in Fig. 4 and was also confirmed quantitatively. Therefore, only the high-statistics data set taken at 546 MeV beam is discussed in the following.

## III. POPULATION OF THE $2^+_{\rm ms}$ CANDIDATE RELATIVE TO THE $2_1^+$ STATE

In order to assess the population of the $2^+_{\rm ms}$ candidate relative to the $2_1^+$ state, it is not sufficient to regard the observed $\gamma$-ray intensities discussed in the previous section. This is because the intensity of the $2_1^+ \rightarrow 0^+_{gs}$ transition includes not only the cases where the $2_1^+$ state was populated directly by the $\alpha$ transfer, but also the cases where the $2_1^+$ state was fed by higher-lying states such as the $4_1^+$, $3_1^-$, $2_2^+$ states, etc. Consequently, the observed $2_1^+ \rightarrow 0^+_{gs}$ intensity has to be purged from feeding before comparison to the observed intensity of the $2^+_{\rm ms}$ candidate decays.

The transitions feeding the $2_1^+$ state were identified from $\gamma$-$\gamma$ coincidence data with a gate on the $2_1^+ \rightarrow 0^+_{gs}$ transition at 602.3 keV. All of them are marked in Fig. 4. The $4_1^+ \rightarrow 2_1^+$ transition at 528.3 keV and the $6_1^+ \rightarrow 4_1^+$ transition at 529.7 keV cannot be separated in the $\gamma$-ray spectrum within the resolution after Doppler correction of 4.0(1) keV FWHM at 530 keV. The full intensity of the doublet peak near 530 keV contains the intensity of both transitions. Since the $6_1^+$ state

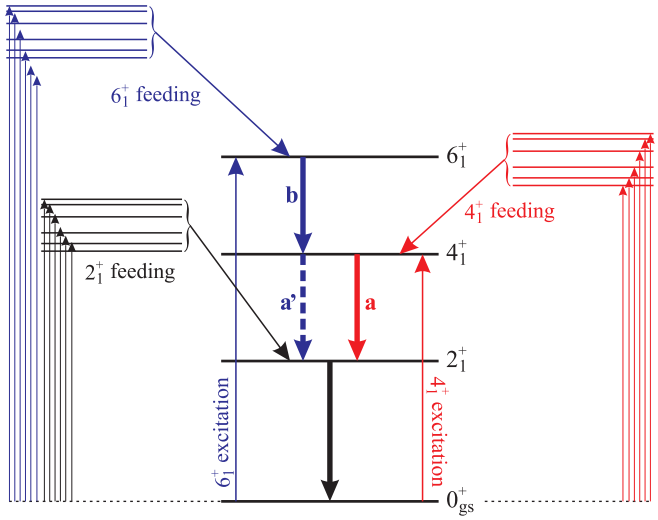


FIG. 5. (Color online) Schematic level scheme with the states and transitions relevant for the analysis of the $2^+_1$ level feeding. The $4^+_1 \to 2^+_1$ and the $6^+_1 \to 4^+_1$ transitions form a doublet in the $\gamma$-ray spectrum that cannot be resolved. This doublet contains the intensities from the direct population of the $4^+_1$ state by the $\alpha$ transfer and its population from all higher-lying states except for the $6^+_1$ state (red part of the figure, transition **a**), the decay of the $4^+_1$ state fed by the $6^+_1$ state (blue, dashed arrow, transition **a′**), as well as the decays of the $6^+_1$ state, populated directly by the $\alpha$ transfer or from higher-lying states (remaining blue part, transition **b**). Further transitions feed the $2^+_1$ state (left). See text for details.

decays exclusively to the $4^+_1$ state, only the intensity of the $4^+_1 \to 2^+_1$ transition is relevant for the feeding analysis. However, the relative intensities of the $4^+_1 \to 2^+_1$ and the $6^+_1 \to 4^+_1$ transition in the doublet can be obtained from $\gamma$-$\gamma$ coincidence data. Feeding of the MSS candidate by $\gamma$ decays of higher-lying states has not been observed. A schematic level scheme with the relevant states and transitions is shown in Fig. 5. The sum of transitions **a** and **a′** in Fig. 5, i.e., the total intensity $I_{a+a'}$ of the $4^+_1 \to 2^+_1$ transition, is relevant for the feeding analysis as mentioned before. The total intensity of the doublet $I_{\text{doublet}} = I_{a+a'+b}$ contains the transitions **a**, **a′**, and **b** in Fig. 5. Hence, the intensity $I_b$ of the $6^+_1 \to 4^+_1$ transition (transition **b**) has to be determined. Since transition **a′** contains only those decays of the $4^+_1$ state where it was fed by the $6^+_1$ state, $I_{a'} = I_b$.

Let $I_{x|y}$ be the intensity of transition $x$ obtained from $\gamma$-$\gamma$ coincidence data with a gate on transition $y$. Then, the intensity in the doublet after putting a gate on the $2^+_1 \to 0^+_{gs}$ transition is given by

$$\begin{aligned} I_{\text{doublet}|2^+_1\to 0^+_{gs}} &= I_{a|2^+_1\to 0^+_{gs}} + I_{a'|2^+_1\to 0^+_{gs}} + I_{b|2^+_1\to 0^+_{gs}} \\ &= I_{a|2^+_1\to 0^+_{gs}} + 2I_{b|2^+_1\to 0^+_{gs}}. \end{aligned} \quad (3)$$

When a gate is put on the doublet itself, the transitions **a′** (coincident with **b**) and **b** (coincident with **a′**) can be accessed at the location of the doublet. The transition **a** excludes the cases where the $4^+_1$ state has been fed by the $6^+_1$ state. Hence, transition **a** is not coincident with transition **a′** or **b** and does not appear when a gate is set on the doublet. Therefore,

$$\begin{aligned} I_{\text{doublet}|\text{doublet}} &= I_{a'|\text{doublet}} + I_{b|\text{doublet}} \\ &= 2I_{b|\text{doublet}}. \end{aligned} \quad (4)$$

The contribution of the $4^+_1$ decay to the total doublet intensity can be obtained from Eqs. (3) and (4) when taking into account the $\gamma$-ray detection efficiencies $\epsilon_\gamma$ for the transitions that were gated on

$$\frac{I_{4^+_1\to 2^+_1}}{I_{\text{doublet}}} = \frac{I_{a+a'}}{I_{\text{doublet}}} = 1 - \frac{\epsilon_{2^+_1\to 0^+_{gs}}}{2\epsilon_{\text{doublet}}} \frac{I_{\text{doublet}|\text{doublet}}}{I_{\text{doublet}|2^+_1\to 0^+_{gs}}}. \quad (5)$$

The detection efficiencies were determined from known relative $\gamma$-ray intensities of a $^{152}$Eu calibration source located at the target position. With the aid of Eq. (5), the fraction of the total $4^+_1 \to 2^+_1$ transition in the doublet at 530 keV can be determined to be $I_{4^+_1\to 2^+_1}/I_{\text{doublet}} = 70.6 \pm 2.1\%$.

Using the relative intensities listed in Table I and the ratio $I_{4^+_1\to 2^+_1}/I_{\text{doublet}}$, the degree to which the $2^+_1$ state is fed by higher-lying states can be inferred under the assumptions that all direct feeders of the $2^+_1$ state are accounted for. No other transitions feeding the $2^+_1$ state than those listed in Table I were identified in the available $\gamma$-$\gamma$ coincidence data. Under these assumptions, the population of the candidate for the $2^+_{ms}$ state relative to the population of the $2^+_1$ state is 10.4(10)%. Both decay branches of the $2^+_{ms}$ candidate, i.e., the transitions $2^+_{3\,(ms)} \to 2^+_1$ and $2^+_{3\,(ms)} \to 0^+_{gs}$, have been considered. If any direct feeders of the $2^+_1$ state have been missed here, the quoted relative population represents a lower limit.

TABLE I. Relevant relative transition intensities from the analysis of $\gamma$-ray singles spectra at 546 MeV beam energy: Intensity of the $2^+_1 \to 0^+_{gs}$ transition (normalized to 100.0), intensities of the decays of the candidate for the $2^+_{ms}$ state, and intensities of transitions feeding the $2^+_1$ state. The $4^+_1 \to 2^+_1$ and the $6^+_1 \to 4^+_1$ transitions form a doublet that cannot be resolved. Their relative intensity is obtained from the analysis of $\gamma$-$\gamma$ coincidence data (see text for details). The level energies are taken from [19].

| Transition | Initial state energy (keV) | Intensity |
|---|---|---|
| $2^+_1 \to 0^+_{gs}$ | 602.4 | 100.0(5) |
| $4^+_1 \to 2^+_1 / 6^+_1 \to 4^+_1$ | 1130.6/1660.3 | 79.7(5) |
| $2^+_2 \to 2^+_1$ | 1510.7 | 7.6(2) |
| $3^-_1 \to 2^+_1$ | 1802.9 | 5.1(2) |
| $2^+_{3\,(ms)} \to 2^+_1$ | 1993.7 | 2.2(1) |
| $2^+_{3\,(ms)} \to 0^+_{gs}$ | 1993.7 | 0.5(1) |
| $3^{(+)} \to 2^+_1$ | 2138.2 | 1.2(1) |
| $2^+_4 \to 2^+_1$ | 2237.2 | 1.9(1) |

## IV. DISCUSSION

The only candidate for the $2^+_{ms}$ state of $^{140}$Ba is the $2^+_3$ state at 1993.7 keV excitation energy [8]. This assignment is based on its small $E2/M1$ multipole mixing ratio $\delta = 0.18^{+0.05}_{-0.06}$ determined in $\beta$-decay measurements [19]. Furthermore, the level energy is consistent with the systematics of $2^+_{ms}$ states in nearby nuclei [21]. No other $2^+$ state with spectroscopic

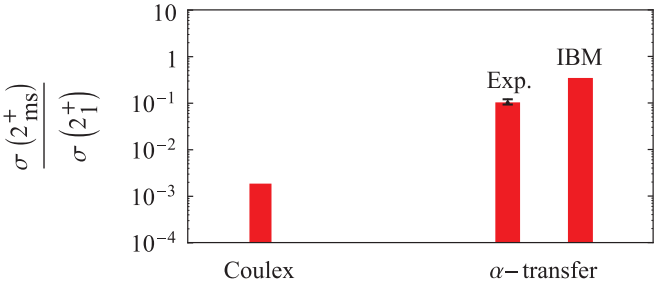


FIG. 6. (Color online) Cross section ratio for population of the $2^+_1$ and $2^+_{ms}$ states of $^{140}$Ba by Coulomb excitation (Coulex) and $\alpha$ transfer. See text for details.

properties indicating mixed-symmetric character is otherwise known in $^{140}$Ba [19].

The population of the MSS candidate by $\alpha$ transfer measured in this work is 10.4(10)% relative to the $2^+_1$ state. This is a factor of 3 lower than the prediction by Alonso *et al.* of a relative population of the MSS in $^{140}$Ba of 1/3 of the $2^+_1$ state [7]. A strong fragmentation of the MSS can be ruled out, since no other $2^+$ state with suitable decay characteristics has been found at nearby energies.

Besides the $2^+_3$ state, the $2^+_2$ state of $^{140}$Ba at 1510.7 keV excitation energy is strongly populated by the $\alpha$-transfer reaction with an intensity of 25.6(19)% relative to the $2^+_1$ state (feeding of the $2^+_2$ state from higher-lying states has been accounted for). This strong population is close to the prediction for the MSS by Alonso *et al.*, yet the $2^+_2$ state can be ruled out as the $2^+_{ms}$ state due to the strong $E2$ component of its decay to the $2^+_1$ state ($\delta = -0.6^{+0.18}_{-0.17}$ [19]), its missing decay branch to the ground state and its excitation energy not fitting the systematics of MSSs in nearby nuclei.

In Fig. 6, the observed and predicted population of the (only candidate for the) MSS of $^{140}$Ba by $\alpha$ transfer relative to the $2^+_1$ state is compared to the same ratio for Coulomb excitation of the $2^+_{ms}$ and $2^+_1$ states of $^{140}$Ba. For the calculation of the Coulomb excitation cross section, the value of the matrix elements for the $2^+_1$ state from [22] were used, and for the $2^+_{ms}$ state the value $B(E2,0^+_1 \rightarrow 2^+_{ms}) \approx 0.75$ W.u. was calculated according to the expression given in [23] for the U(5) limit of IBM-2. A "safe" bombarding energy of 411 MeV was assumed according to Cline's criterion [24]. Clearly, the MSS is much more strongly excited relative to the $2^+_1$ state by $\alpha$ transfer than by Coulomb excitation. Due to this strong relative population of the $2^+_{ms}$ state, the $\alpha$-transfer reaction can serve as a valuable tool to study the decay properties of MSSs in radioactive nuclei by experiments employing stable ions beams, although the cross section for the excitation of the $2^+_1$ state by $\alpha$ transfer is significantly lower than by Coulomb excitation. In the case of $\alpha$-transfer experiments, MSS can also be identified without the information on transition strengths that is obtained in Coulomb excitation experiments. $M1$ transition strengths of MSS candidate decays to the fully symmetric $2^+$ state could be determined by the measurement of the $2^+_{ms}$ level lifetime, e.g., by the Doppler-shift attenuation method (DSAM), and the determination of the transition's multipole mixing ratio via the analysis of $\gamma$-ray angular distributions.

## V. CONCLUSIONS

Strong population of the MSS in $^{140}$Ba by $\alpha$ transfer was observed, yet not as strong as predicted by Alonso *et al.* [7]. This assumes that the only candidate for the $2^+_{ms}$ state indeed is the mixed-symmetry state. That another $2^+$ state is the $2^+_{ms}$ state or that the MSS is strongly fragmented can be ruled out by the available spectroscopic data. Besides the candidate for the $2^+_{ms}$ state, the $2^+_2$ state was nearly as strongly populated by $\alpha$ transfer as predicted for the MSS. However, the $2^+_2$ state can be ruled out as the $2^+_{ms}$ state. Hence, strong population of a $2^+$ state by $\alpha$ transfer cannot serve as a unique signature for the mixed-symmetric character of the state. Nevertheless, $\alpha$ transfer can serve as a useful reaction mechanism for the study of the decay properties of MSSs of some radioactive isotopes in experiments with stable ion beams.

## ACKNOWLEDGMENTS

We thank the accelerator crew of the Laboratori Nazionali di Legnaro for providing the xenon beam, and K.-H. Speidel, A. Vitturi, O. Möller, G. Rainovski, and V. Werner for fruitful discussions. This work was supported by HIC for FAIR and the German BMBF under Grants No. 05P09RDFN4 and No. 05P12RDFN8. A. Gadea has been supported by MINECO, Spain, under the grant FPA2014-57196-C5, Generalitat Valenciana, Spain, under the grant PROMETEOII/2014/019, and by the EU under the FEDER program.

[1] F. Iachello, Phys. Rev. Lett. **53**, 1427 (1984).
[2] N. Pietralla, P. von Brentano, and A. Lisetskiy, Prog. Part. Nucl. Phys. **60**, 225 (2008).
[3] A. Arima, T. Otsuka, F. Iachello, and I. Talmi, Phys. Lett. B **66**, 205 (1977).
[4] T. Otsuka, A. Arima, F. Iachello, and I. Talmi, Phys. Lett. B **76**, 139 (1978).
[5] T. Ahn, L. Coquard, N. Pietralla, G. Rainovski, A. Costin, R. Janssens, C. Lister, M. Carpenter, S. Zhu, and K. Heyde, Phys. Lett. B **679**, 19 (2009).
[6] C. Walz, H. Fujita, A. Krugmann, P. von Neumann-Cosel, N. Pietralla, V. Y. Ponomarev, A. Scheikh-Obeid, and J. Wambach, Phys. Rev. Lett. **106**, 062501 (2011).
[7] C. E. Alonso, J. M. Arias, L. Fortunato, N. Pietralla, and A. Vitturi, Phys. Rev. C **78**, 017301 (2008).
[8] W. D. Hamilton, A. Irbäck, and J. P. Elliott, Phys. Rev. Lett. **53**, 2469 (1984).
[9] J. R. Vanhoy, J. M. Anthony, B. M. Haas, B. H. Benedict, B. T. Meehan, S. F. Hicks, C. M. Davoren, and C. L. Lundstedt, Phys. Rev. C **52**, 2387 (1995).
[10] S. F. Hicks, C. M. Davoren, W. M. Faulkner, and J. R. Vanhoy, Phys. Rev. C **57**, 2264 (1998).
[11] O. Kenn, K.-H. Speidel, R. Ernst, S. Schielke, S. Wagner, J. Gerber, P. Maier-Komor, and F. Nowacki, Phys. Rev. C **65**, 034308 (2002).
[12] M.-C. Lemaire, Phys. Rep. **7**, 279 (1973).

[13] A. Astier, P. Petkov, M.-G. Porquet, D. S. Delion, and P. Schuck, Phys. Rev. Lett. **104**, 042701 (2010).
[14] J. Leske, K.-H. Speidel, S. Schielke, O. Kenn, J. Gerber, P. Maier-Komor, S. J. Q. Robinson, A. Escuderos, Y. Y. Sharon, and L. Zamick, Phys. Rev. C **71**, 044316 (2005).
[15] S. Akkoyun *et al.*, Nucl. Instrum. Methods A **668**, 26 (2012).
[16] A. Gadea *et al.*, Nucl. Instrum. Methods A **654**, 88 (2011).
[17] A. Venturelli and D. Bazacco, LNL Annual Report 2004 (unpublished), p. 220.
[18] A. Lopez-Martens, K. Hauschild, A. Korichi, J. Roccaz, and J.-P. Thibaud, Nucl. Instrum. Methods A **533**, 454 (2004).
[19] N. Nica, Nucl. Data Sheets **108**, 1287 (2007).
[20] A. Illana *et al.*, Phys. Rev. C **89**, 054316 (2014).
[21] T. Möller, Ph.D. thesis, Technische Universität Darmstadt, 2014 (unpublished).
[22] C. Bauer *et al.*, Phys. Rev. C **86**, 034310 (2012).
[23] P. van Isacker, K. Heyde, J. Jolie, and A. Sevrin, Ann Phys. (N.Y.) **171**, 253 (1986).
[24] D. Cline, Bull. Am. Phys. Soc. **14**, 726 (1969).